Water Practice & Technology

IWA PUBLISHING

Water Practice & Technology Vol 18 No 4, 911 doi: 10.2166/wpt.2023.041

Artemisia stelleriana-mediated ZnO nanoparticles for textile dye treatment: a green and sustainable approach

Juhi Puthukulangara Jaison and Joseph Kadanthottu Sebastian *

Department of Life Sciences, Christ University, Bangalore, Karnataka 560029, India
*Corresponding author. E-mail: joseph.ks@christuniversity.in

JKS, 0000-0003-4384-2462

ABSTRACT

Textile effluents being one of the major reasons for water pollution raises major concern for water bodies and the habitation surrounding them. The lack of biologically safer treatment solutions creates a major concern for the disposal of these effluents. The present study focuses on the degradation of textile dyes using leaf extract of *Artemisia stelleriana*-assisted nanoparticles of zinc oxide (ZnO-NPs). ZnO NPs synthesized were confirmed using spectroscopic, X-ray diffraction and microscopic analysis. The current research utilizes widely used major textile dyes, Reactive Yellow-145 (RY-145), Reactive Red-120 (RR-120), Reactive Blue-220 (RB-220) and Reactive Blue-222A (RB-222A), which are released accidentally or due to the non-availability of cost-efficient, dependable and environment-friendly degradation methods, making this work a much-needed one for preventing the discharge before treatment. The biosynthesized ZnO-NPs were top-notch catalysts for the reduction of these dyes, which is witnessed by a gradual decrease in absorbance maximum values. After 320 min, ZnO-NPs under UV light exposure showed 99, 95, 94 and 45% degradations of RY-145, RR-120, RB-220 and RB-222A dyes, respectively. The phytotoxicity study conducted at two trophic levels revealed that the A. *stelleriana*-mediated ZnO-NPs have great potential for the degradation of textile dyes, allowing them to be scaled up to large-scale treatments.

Key words: *Artemisia stelleriana*, photocatalytic degradation, phytotoxicity, textile dyes, water treatment, zinc oxide nanoparticles

HIGHLIGHTS

- Zinc nanoparticles were synthesized using *Artemisia stelleriana* leaves.
- Near-spheroid, thin rods and irregular nanoparticles were detected.
- A band gap of 3.033 eV was obtained.
- Degradations of Reactive Yellow-145, Reactive Red-120, Reactive Blue-220 and Reactive Blue-222A dyes were validated owing to the photocatalytic activity of ZnO nanoparticles.
- Low toxicity was observed during the toxicity analysis of the degraded dye.

GRAPHICAL ABSTRACT

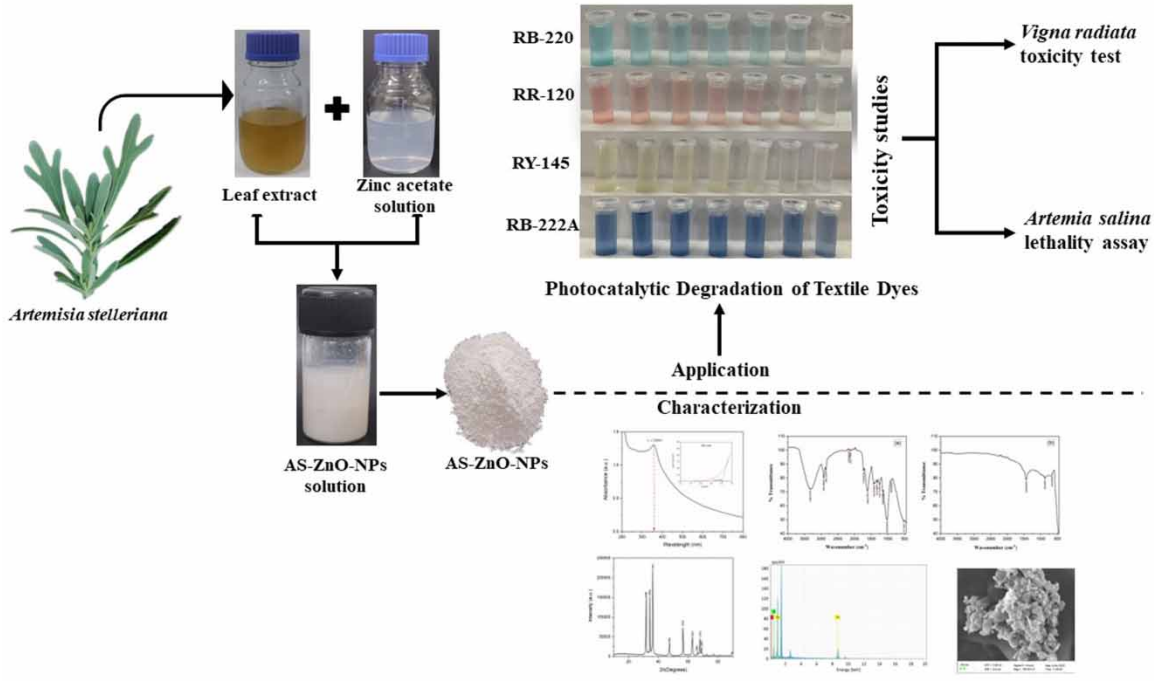

INTRODUCTION

The equilibrium between economic sustainability and environmental deterioration is also an evident reason for pollution and waste management (Dave *et al.* 2021). Water pollution is a growing concern due to industrial waste. Among all the industrial effluents, one of the major reasons for pollution is synthetic dyes, which are utilized in textile industries (Carneiro *et al.* 2010). These dyes are carcinogenic and cannot be degraded naturally (Ito *et al.* 2016). Textile wastewater is increasing day by day due to the enormous production of fabric products (Gita *et al.* 2017). The discharge of textile effluent decreases water quality, making it impossible to use water directly for industrial purposes or drinkable water (through desalination) (Panagopoulos 2021, 2022; Panagopoulos & Giannika 2022). According to the World Bank report, about 20% of industrial wastewater production arises from the textile industries. Accidental dumping and discharging of dye effluents into the water bodies are questioning the quality of water resources (Rafiq *et al.* 2021).

The presence of dye in the water resources can disturb the ecosystem by preventing sunlight penetration into the surface of the water and it also can cause various human diseases (Khan & Malik 2018). Physical, chemical and biological processes have attained the degradation of these dyes from textile industries. Although these processes are costly and time-consuming, nanoparticle-mediated photocatalytic degradation of dyes is an emerging idea in this era. In photocatalytic degradation, the carcinogenic dyes are degraded by biosynthesized nanocatalysts under the influence of light irradiation. When compared with the conventional methods, this approach is less expensive and does not produce any polycyclic products (Nagajyothi *et al.* 2020). Earlier studies reported that zinc oxide nanoparticles (ZnO-NPs) could be utilized as excellent photocatalysts in the degradation of textile dyes due to their high stability, large surface area and electron-binding energy (Osuntokun *et al.* 2019).

Artemisia stelleriana (AS), also known as 'dusty miller' or 'old woman' or 'beach wormwood' is an aromatic herb with high medicinal value, due to the presence of monoterpenes, sesquiterpenes, flavonoids and other compounds (Mayuri *et al.* 2022). The leaves of AS are used to treat various ailments, including peptic ulcers, hair loss, stimulation of mental faculties and carminatives. AS contains alkaloids, vitamins A, B1, B2 and C and minerals. They also contain various other substances, such as coumarin derivatives, which were used as an effective antioxidant and anticarcinogen (Mucciarelli & Maffei 2001). To the best of our information, this is the first attempt to synthesize zinc nanoparticles from AS. In addition, the research utilizes widely used major textile dyes (RY-145, RR-120, RB-220 and RB-222A), which are released accidentally or due to the non-availability of cost-efficient,

dependable and environment-friendly degradation methods, making this work a much-needed one for preventing the discharge before treatment.

In the present study, biologically synthesized ZnO-NPs using leaf extract of AS were utilized for the photocatalytic activity of textile dyes and the phytotoxicity tests were performed on degraded dye using representative samples to analyse the toxic levels by the degraded compounds.

MATERIALS AND METHODS

Materials

Plantlets of AS identified and collected from the Foundation for Revitalization of Local Health Traditions (FRLHT) Bangalore, India were raised in greenhouse conditions. Zinc acetate dihydrate and sodium hydroxide were procured from Himedia Laboratories, India. Reactive Yellow-145 (RY-145, Cas no. 93050-80-7), Reactive Red-120 (RR-120, Cas no. 61951-82-4), Reactive Blue-220 (RB-220, Cas no. 128416-19-3) and Reactive Blue-222A (RB-222A, Cas no. 93051-44-6) dyes were procured from Itesh Enterprises (Jetpur, India).

Plant extract preparation

The preparation of plant extract followed the previous protocols with a few minor modifications (Umamaheswari *et al.* 2021). Fresh leaves were weighed (10 g) and ground in a mortar and pestle. The ground leaves were heated to 60 °C and refluxed for 30 min in 50 mL of distilled water. The aqueous leaf extract was filtered and kept at 4 °C for future analysis after cooling to room temperature (RT).

Nanoparticles synthesis

ZnO-NPs were synthesized using the given article (Mohammadi Shivyari *et al.* 2022) with some modifications. Aqueous extract of AS was mixed with 0.1 M zinc acetate solution, which was constantly stirred using a magnetic stirrer at RT for 15 min. The pH (10) was adjusted using 2 M NaOH solution. A white dispersion was obtained, centrifuged at 10,000 rpm for 15 min and the pellet was washed thrice in sterile distilled water and ethanol. The pellet obtained was dried at 80 °C. The obtained AS-mediated ZnO-NPs (AS-ZnO-NPs) were calcinated at 550 °C for 2 h in a muffle furnace. The prepared material characterized by Fourier-transform infrared spectroscopy (FTIR) analysis and X-ray powder diffraction (XRD) study.

Characterization of AS-ZnO-NPs

The AS-ZnO-NPs were characterized using a UV-Vis spectrophotometer (Shimadzu, Japan) from the range of 200–800 nm. Chemical groups involved in the synthesis of AS-ZnO-NPs were determined using attenuated total reflection FTIR (ATR–FTIR) (Shimadzu, Japan), verified at 400–4,000 cm^{-1}. Elemental mapping and surface morphology were analysed using energy dispersing X-ray analysis (EDX) and Field emission scanning electron microscopy (FESEM). The crystalline nature of the sample was determined using XRD (Miniflex, Rigaku, Japan) analysis.

Degradation of textile dyes

The photocatalytic degradation of textile dyes- RY-145, RR-120, RB-220 and RB-222A, under UV light irradiation was carried out as given in the literature (Kaur *et al.* 2021) with slight modifications. 20 mL of each of the 5 mg/L dye solutions was utilized for the experiment. For each of the dye solutions, 20 mg of freshly prepared AS-ZnO-NPs were mixed. The reaction mixture was stirred for 10 min in dark conditions to ensure thorough dispersion. The test solutions were exposed to UV light and stirred continuously and the percentage of degradation was observed at specific time intervals (0, 10, 20, 40, 80, 160 and 320 min) by measuring the absorbance value using a UV-Vis spectrophotometer in the range of 300–700 nm. The maximum absorbance peaks of RR-120, RY-145, RB-222A and RB220 dyes were at 506, 407, 600 and 666 nm, respectively. The degradation was observed by decreased absorbance values. Based on the observations, the photocatalytic degradation efficiency of AS-ZnO-NPs was determined using the following equation (Yashni *et al.* 2020).

$$\% \text{ degradation} = (A_0/A)/A \times 100 \quad (1)$$

where A_0 is the initial absorbance of the dye solution and A is the final absorbance of the dye solution.

Phytotoxicity assay

The AS-ZnO-NPs degradation efficiency and phytotoxicity reduction of treated dyes were analysed using the *Vigna radiata* toxicity study and the Brine shrimp lethality assay. The *V. radiata* toxicity study was carried out

as previously described (Dharshini *et al.* 2021) with slight modifications. The seeds were germinated in a Petri dish (10 seeds each, 1 cm spacing) and subjected to treated and untreated dyes and AS-ZnO-NPs solutions, respectively. The plant's shoot and root length toxicity were calculated after 7 days of treatment. The Brine shrimp (*A. salina*) lethality assay was performed using a previously established method (Bilal *et al.* 2016) with slight modifications. 10 nauplii each were cultured for 24 h at RT with treated and untreated dye and AS-ZnO-NPs solutions, respectively. The Mortality Rate (MR) was calculated by counting the dead nauplii under a binocular microscope.

RESULTS AND DISCUSSION

Synthesis and UV-Vis studies of AS-ZnO-NPs

Phytochemicals play a vital role in reducing and stabilizing nanoparticles and can reduce the zinc ions in solution to ZnO-NPs. In an alkaline medium, the mixture of AS phytochemicals and zinc acetate showed a colour change from a greenish-yellow solution to a white precipitate dispersion (Figure 1), indicating the formation of AS-ZnO-NPs. The UV-Vis spectral image of AS-ZnO-NPs colloidal solution was observed from 200 to 800 nm and a peak was obtained at 358 nm (Figure 2), which is specific for ZnO nanoparticles. The result is concurrent with earlier studies (Chen *et al.* 2019). This peak value was used to calculate the band gap energy from the Tauc equation. A sharp band gap of 3.033 eV was obtained from the graph. The smaller band gap will easily excite the electrons from the valance band to the conduction band, which will support photocatalytic activity, leading to the degradation of dyes.

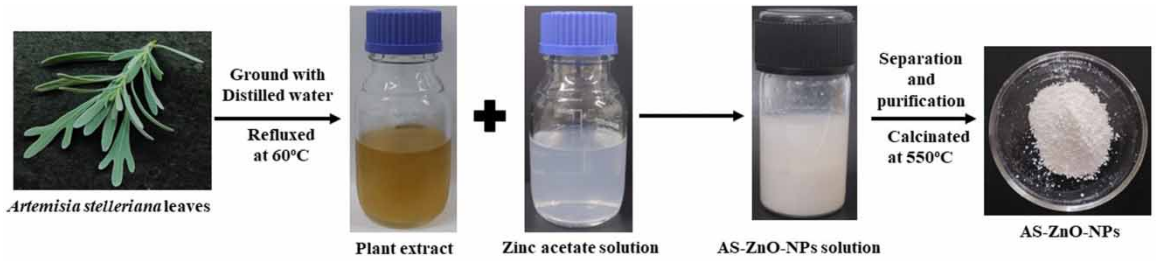

Figure 1 | Flowchart showing the synthesis of AS-ZnO-NPs by using *A. stelleriana* leaves.

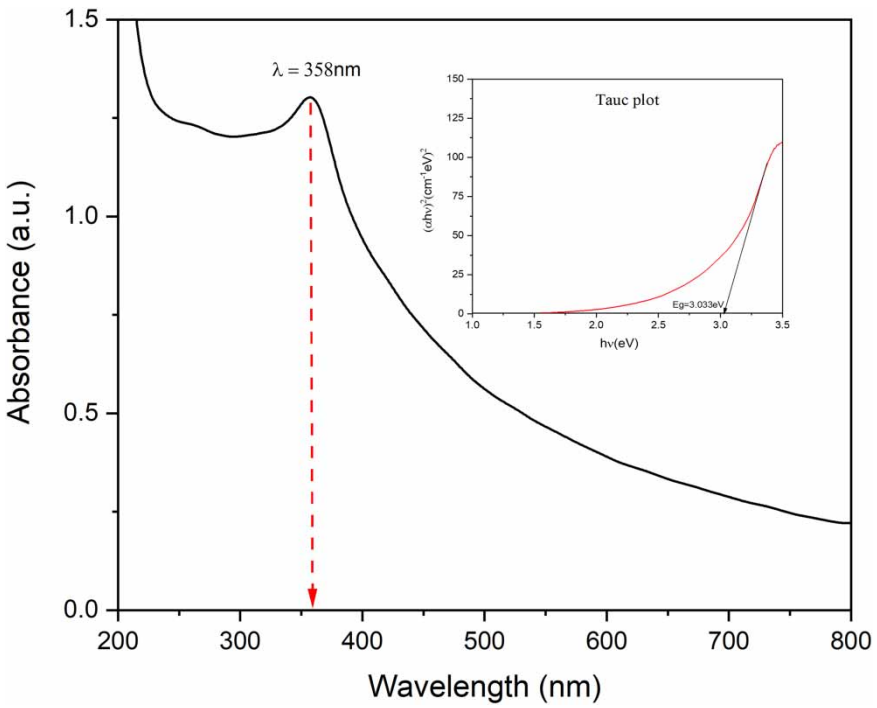

Figure 2 | UV-Vis spectra of biologically synthesised AS-ZnO-NPs by using *A. stelleriana* leaves.

FTIR spectra of ZnO-NPs

The FTIR spectrum identifies plant molecules involved in the reduction and stabilization of zinc salt to nanoparticles. The spectrum of the plant (Figure 3(a)) and synthesized ZnO-NPs (Figure 3(b)) was observed in the range between 400 and 4,000 cm^{-1}. The biosynthesized AS-ZnO-NPs showed a peak at 661.84 cm^{-1} attributed to the metal-oxygen bond, which could be due to zinc and oxygen bonding vibrations (Nimbalkar & Patil 2017), confirming the synthesis. In addition, peaks were observed at 1,435.40 and 874.30 cm^{-1} due to carboxylic (O–H bending) acid and C = C bending. The AS sample showed peaks from 3,328.23 to 517.18 cm^{-1}, which are associated with alkaloids, flavonoids and phenolic compounds, respectively, (Kamarajan *et al.* 2022) suggesting the utilization of phytochemical constituents in the reduction of zinc ions to ZnO nanoparticles. As previously reported, the phytochemicals present in the plant extract synthesize the ZnO-NPs by the following mechanisms: (1) Reduction of Zn salt to Zn followed by addition of oxygen during calcination where few phytochemicals stabilize the nanoparticles and (2) formation of Zn^{2+} complex followed by hydrolysis leading to $Zn(OH)_2$ and ultimately the formation of Zn nanoparticles by calcination (Mutukwa *et al.* 2022).

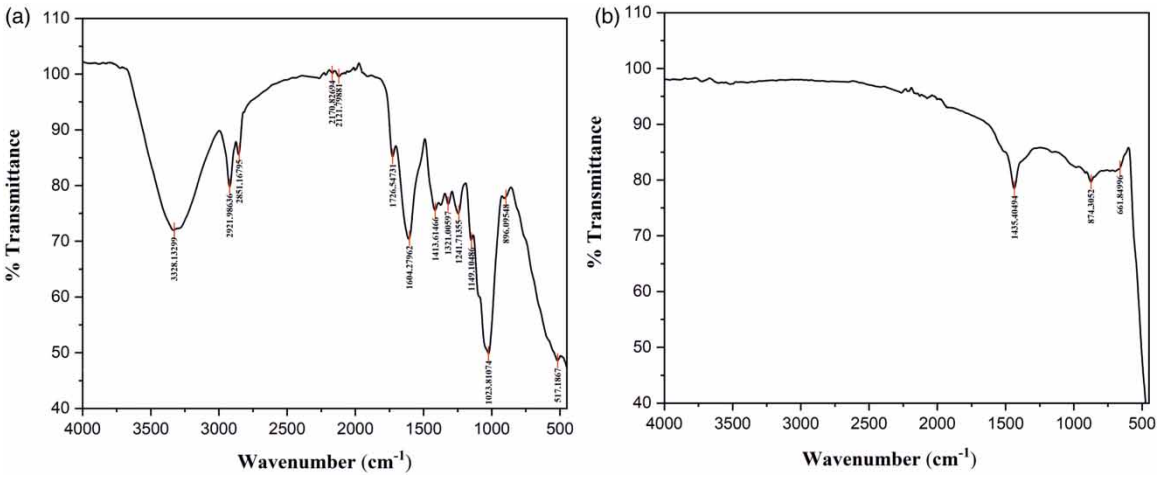

Figure 3 | FTIR spectra of (a) functional groups present in plant extract and (b) functional groups utilized and reduced during the synthesis of AS-ZnO-NPs.

FESEM and EDX

The morphology of the AS-ZnO-NPs was observed at different magnifications using FESEM. SEM analysis showed polymorphic ZnO nanoparticles in dimensions of 10–100 nm. AS-ZnO-NPs displayed near-spheroid, thin rod and irregular shapes (Figure 4). Similar observations were made in lemon fruit-based ZnO nanoparticles (Hossain *et al.* 2019). The agglomerated and differently shaped nanoparticles were also reported in ZnO-NPs

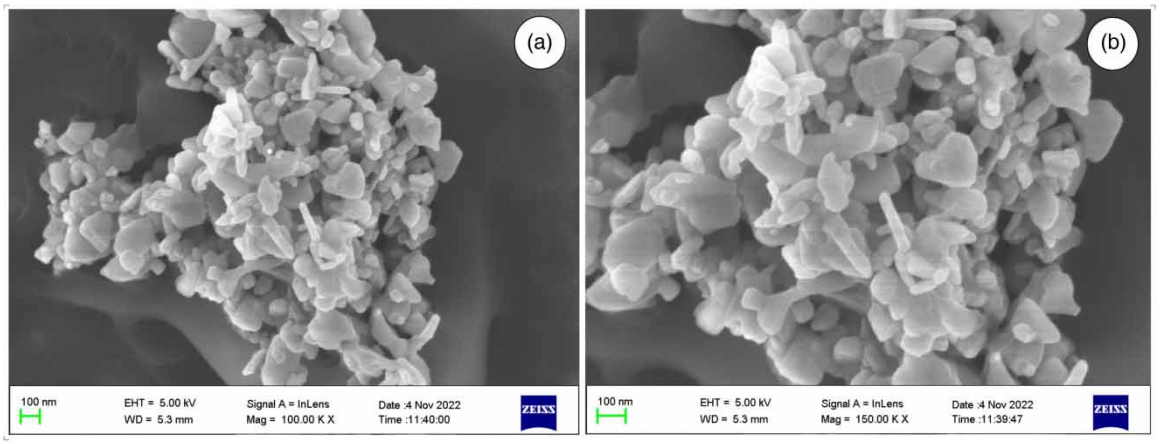

Figure 4 | Characterization of biogenic AS-ZnO-NPs by SEM analysis (a) 100× and (b) 150 × .

synthesized using *Syzygium cumini* (Sadiq *et al.* 2021). The EDX spectra displayed the synthesized nanoparticles containing elements like zinc, oxygen and carbon (Figure 5). The spectra showed two robust peaks at 1 and 8.7 keV for zinc and a peak at 0.5 keV for oxygen, which are distinctive for ZnO nanoparticles as reported in previous studies (Barzinjy & Azeez 2020). The presence of carbon was due to the sample coating during FESEM imaging.

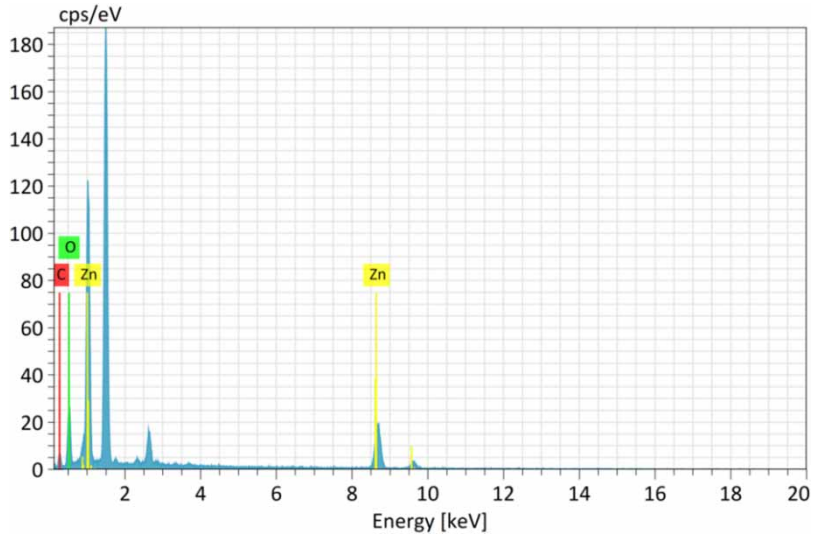

Figure 5 | EDX spectra of synthesized ZnO-NPs.

X-ray powder diffraction

The diffraction pattern of biosynthesized ZnO nanoparticles was identified and shown in Figure 6. Distinctive peaks measured at 2θ values of 31.73°, 34.37°, 36.22°, 47.49°, 56.55°, 62.79°, 67.89° and 69.02° were assigned to the planes of ZnO, i.e. (100), (002), (101), (102), (110), (103), (200), (112) and (201), respectively all peaks were characteristic AS-ZnO-NPs suggesting high purity and the crystalline nature of the nanoparticles (Khan *et al.* 2021). The peak at 36.22° and their corresponding planes are in concordance with standard hexagonal structure (JCPDS card number – 98-001-1316) and based on the Debye–Scherrer formula, the average crystalline size of the synthesized nanoparticles was calculated to be 22.54 nm. The crystalline size of *A. stelleriana*-mediated ZnO-NPs was smaller than *Calotropis procera* leaves-mediated ZnO-NPs (Gawade *et al.* 2017). Similar reports were seen in ZnO-NPs synthesized using *Myristica fragrans* fruit extract (Faisal *et al.* 2021).

Photocatalytic degradation of dyes

Under UV light, the photocatalytic degradation activity of AS-ZnO-NPs was determined by analysing RY-145, RR-120, RB-220 and RB-222A dyes (Figure 7). The degradation of each dye was recorded at specific time intervals (0, 10, 20, 40, 80, 160 and 320 min) using the UV-Vis spectrophotometer. The findings showed that the synthesized nanoparticles are excellent catalysts for the reduction of RY-145, RR-120, RB-220 and RB-222A, which is confirmed by a falloff in absorbance maximum values. After 320 min of UV light exposure, 99, 95, 94 and 45% degradations were observed in RY-145, RR-120, RB220 and RB-222A dyes, respectively (Figure 7(a)–7(d)). The degradation can be attributed to the sharp band gap of 3.033 eV, which might have excited the electrons from the valance band to the conduction band, leading to electron–hole pairs, which would have eventually led to the formation of superoxide radicals like reactive oxygen species mediating the degradation of dyes (Vinayagam *et al.* 2020). The reusability of the AS-ZnO-NPs was determined using XRD analysis. After the degradation of dyes, the crystalline nature of ZnO-NPs was not altered and also the peak location remains to be same as before the degradation for RY-145, RR-120, RB220 and RB-222A, respectively (Figure 8(a)–8(d)). The result concluded that the AS-ZnO-NPs are reusable and stable. These are in concurrence with the previous reports (Khan *et al.* 2021).

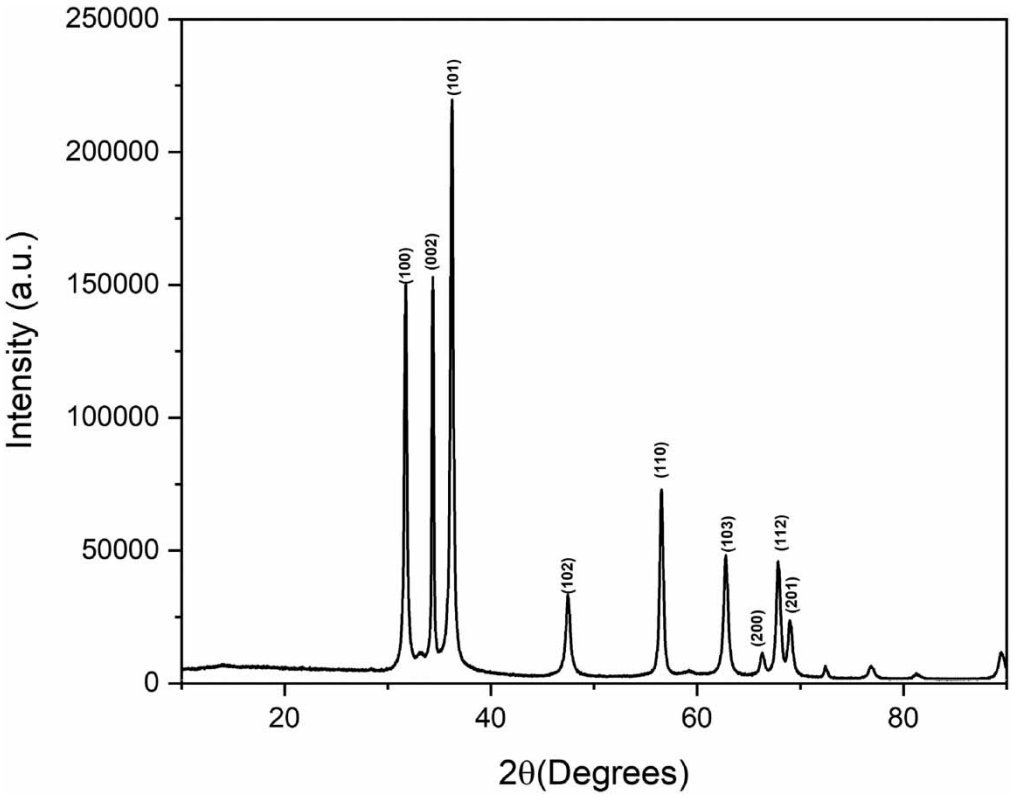

Figure 6 | Characterization of biogenic AS-ZnO-NPs by XRD analysis to elucidate the crystalline structure.

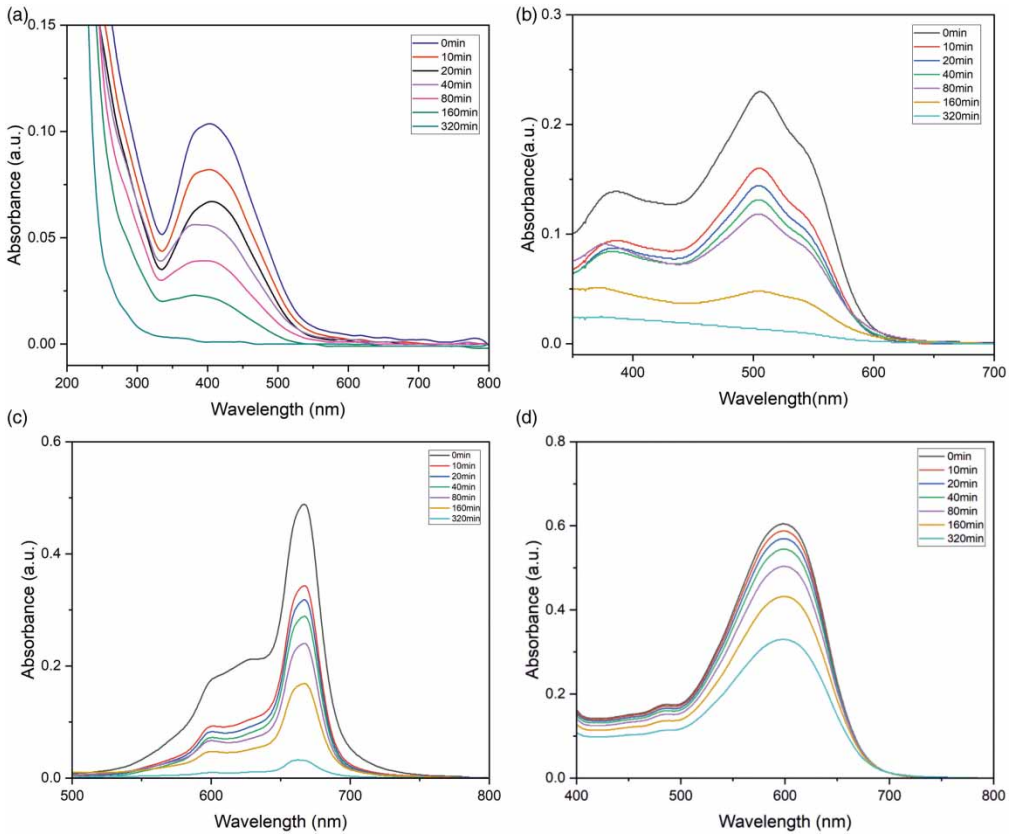

Figure 7 | Photocatalytic degradation of dyes at different time intervals (0–320 min) (a) RY-145; (b) RR-120; (c) RB-220 and (d) RB-222A.

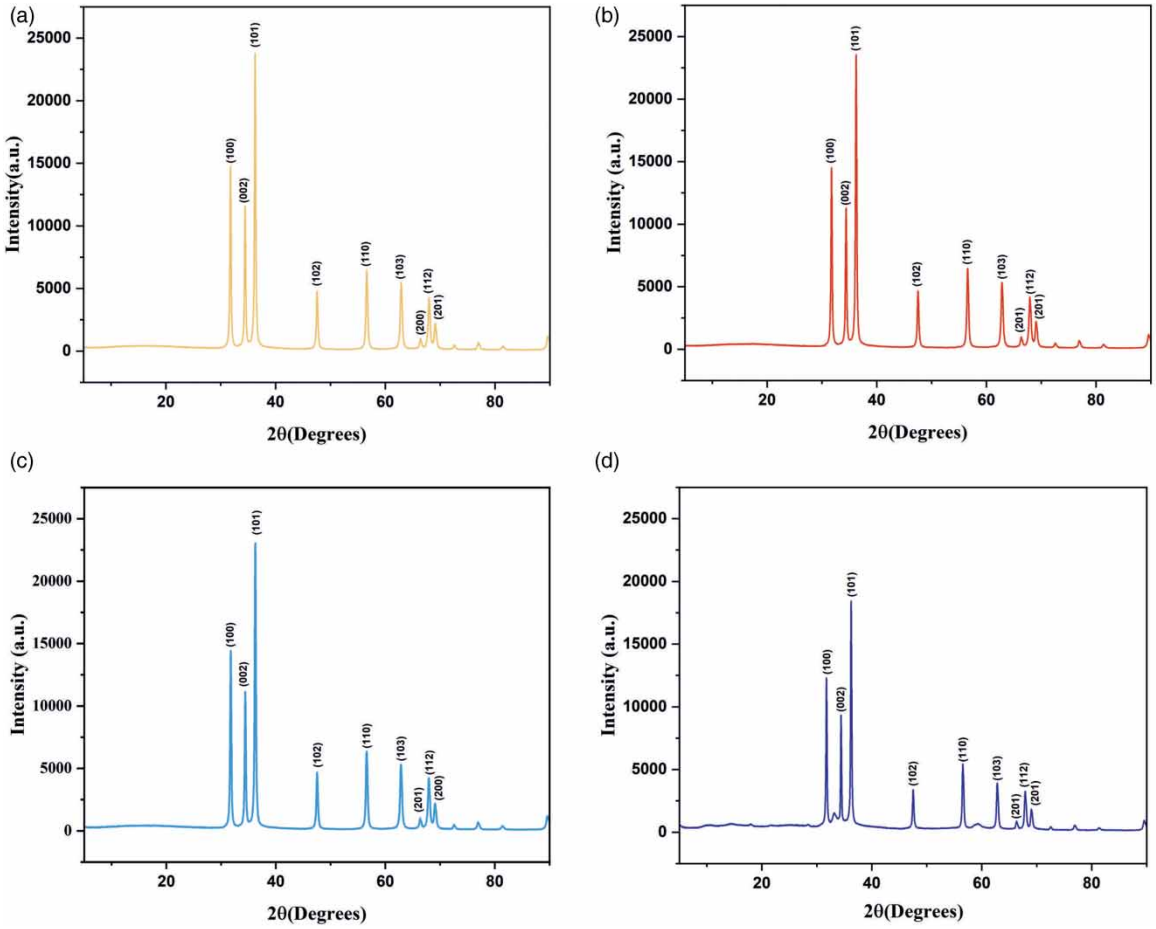

Figure 8 | Characterization of recovered AS-ZnO-NPs by XRD analysis after treatment with different dyes (a) RY-145; (b) RR-120; (c) RB-220 and (d) RB-222A.

Table 1 | Phytotoxicity analysis of the treated dyes

	***V. radiata* toxicity**						***A. salina* mortality**				
	Untreated		**Treated**		**Phytotoxicity reduction (%) after treatment**		**Untreated**		**Treated**		
Dyes	**Root length (cm)**	**Shoot length (cm)**	**Root length (cm)**	**Shoot length (cm)**	**Root length**	**Shoot length**	**Alive nauplii**	**Dead nauplii**	**Alive nauplii**	**Dead nauplii**	**Percentage of mortality (%)**
Distilled water	4.38 ± 0.26	9.04 ± 0.37	4.38 ± 0.26	9.04 ± 0.37	–	–	10 ± 0	0 ± 0	10 ± 0	0 ± 0	0
$KMnO_4$	–	–	–	–	–	–	0 ± 0	10 ± 0	0 ± 0	10 ± 0	100
RB22O	0.54 ± 0.07	3.53 ± 0.1	4.3 ± 0.05	9.61 ± 0.11	87.4	63.2	1 ± 1	9 ± 1	7.3 ± 0.6	3.7 ± 0.6	27
RB-222A	0.52 ± 0.03	4.40 ± 0.22	3.83 ± 0.31	7.52 ± 0.01	86.2	41.4	2 ± 2	8 ± 2	6.3 ± 0.6	2.7 ± 0.6	37
RR120	1.38 ± 0.04	3.21 ± 0.22	4 ± 0.04	10.92 ± 0.04	65.3	70.57	2 ± 1	8.3 ± 1	8.7 ± 0.6	1.3 ± 0.6	13
RY145	0.58 ± 0	2.22 ± 0.03	3.48 ± 0.05	9.44 ± 0.19	83.3	76.4	1 ± 1	9 ± 1	9 ± 1	1 ± 1	10

Note: Values are mean (±) standard deviation; (–) not applicable.

Phytotoxicity analysis

Textile effluents are highly toxic to crops. Phytotoxicity studies have great relevance before and after treatment with nanoparticles. The toxicity study was carried out using *V. radiata*, which has great importance in agriculture. Table 1 indicates that the shoot length and root of the *V. radiata* seed were inhibited when the seeds were allowed to grow in untreated textile effluents. On the other hand, better growth was observed in the treated textile effluents. The increase in shoot length was recorded up to 65.3, 83.3, 86.2 and 87.4% for RR120, RY145, RB-222A and RB220 dyes, respectively. Whereas, the radicle length increased by 70.57, 76.4, 41.4 and 63.2% for RR120, RY145, RB-222A and RB220 dyes, respectively. The result concluded that phytotoxicity had reduced immensely after the treatment. In the present investigation, the treated textile effluent did not show any toxicity signs, so it is concluded that the toxic substance was converted into harmless substances through biodegradation.

A. salina was utilized for the toxicity study, which is a true delegate of the aquatic ecosystem. This is a model organism to determine the short-term toxicity of any ecosystem. The *A. salina lethality assay* is a preferred choice to check the potential to kill *A. salina* nauplii cultured in the laboratory within a certain time limit. After 24 h, it was observed that all the *A. salina* survived in the artificial seawater and a 100% MR was observed in potassium permanganate solution ($KMnO_4$) (0.1 mg/mL). It is also visible that the MR was higher in the untreated dye solution when compared with the treated dye solution. In the treated sample, the maximum MR was observed in RB-222A dye and the least mortality was in RY-145 dye (Table 1). So, it was concluded that ZnO-NPs synthesized from *A. stelleriana* reduced the toxicity of the textile dyes.

CONCLUSION

The AS-ZnO-NPs from the aqueous extract of *A. stelleriana* were successfully synthesized and characterized using spectroscopic, microscopic analyses. The method adopted here is simple, cost-effective, pollution-free and non-toxic. A characteristic peak at 358 nm was observed in UV-Vis spectral analysis and the biomolecules involved were identified using FTIR analysis. The crystalline nature of the synthesized ZnO-NPs was confirmed using XRD analysis. The spheroid, thin rods and irregular shapes of the nanoparticles were confirmed using FESEM. Under UV light irradiation, the synthesized nanoparticles showed maximum degradation for RY145 and the least degradation for RB-222A. The reusability of nanoparticles after degradation was also confirmed using XRD analysis. The toxicity study conducted in *V. radiata and A. salina* also revealed that the ZnO-NPs synthesized from *A. stelleriana* reduced the textile dyes' toxicity. The findings from this investigation can be utilized as a reference for future studies. The ZnO-NPs synthesis and degradation studies are still in their infancy and the treatment of dye combinations along with other contaminants needs to be studied to apply in real industrial wastewater treatment scenarios.

DATA AVAILABILITY STATEMENT

All relevant data are included in the paper or its Supplementary Information.

CONFLICT OF INTEREST

The authors declare there is no conflict.

REFERENCES

Barzinjy, A. A. & Azeez, H. H. 2020 Green synthesis and characterization of zinc oxide nanoparticles using *Eucalyptus globulus Labill.* leaf extract and zinc nitrate hexahydrate salt. *SN Applied Sciences* **2**, 991. https://doi.org/10.1007/s42452-020-2813-1.

Bilal, M., Iqbal, M., Hu, H. & Zhang, X. 2016 Mutagenicity, cytotoxicity and phytotoxicity evaluation of biodegraded textile effluent by fungal ligninolytic enzymes. *Water Science and Technology* **73**, 2332–2344. https://doi.org/10.2166/wst.2016.082.

Carneiro, P. A., Umbuzeiro, G. A., Oliveira, D. P. & Zanoni, M. V. B. 2010 Assessment of water contamination caused by a mutagenic textile effluent/dye house effluent bearing disperse dyes. *Journal of Hazardous Materials* **174**, 694–699. https://doi.org/10.1016/j.jhazmat.2009.09.106.

Chen, L., Batjikh, I., Hurh, J., Han, Y., Huo, Y., Ali, H., Li, J. F., Rupa, E. J., Ahn, J. C., Mathiyalagan, R. & Yang, D. C. 2019 Green synthesis of zinc oxide nanoparticles from the root extract of *Scutellaria baicalensis* and its photocatalytic degradation activity using methylene blue. *Optik* **184**, 324–329. https://doi.org/10.1016/j.ijleo.2019.03.051.

Dave, S., Das, J. & Shah, M. P. 2021 *Photocatalytic Degradation of Dyes: Current Trends and Future Perspectives*. Elsevier https://doi.org/10.1016/B978-0-12-823876-9.00031-7.

Dharshini, R. S., Poonkothai, M., Srinivasan, P., Mythili, R., Syed, A., Elgorban, A. M. & Kim, W. 2021 Nano-decolorization of methylene blue by *Phyllanthus reticulatus* iron nanoparticles: an eco-friendly synthesis and its antimicrobial, phytotoxicity study. *Applied Nanoscience*, 1–11. https://doi.org/10.1007/s13204-021-02002-3.

Faisal, S., Jan, H., Shah, S. A., Shah, S., Khan, A., Akbar, M. T., Rizwan, M., Jan, F., Wajidullah, Akhtar, N., Khattak, A. & Syed, S. 2021 Green synthesis of zinc oxide (ZnO) nanoparticles using aqueous fruit extracts of *Myristica fragrans:* their characterizations and biological and environmental applications. *ACS Omega* **6**, 9709–9722. https://doi.org/10.1021/acsomega.1c00310.

Gawade, V. V., Gavade, N. L., Shinde, H. M., Babar, S. B., Kadam, A. N. & Garadkar, K. M. 2017 Green synthesis of ZnO nanoparticles by using *Calotropis procera* leaves for the photodegradation of methyl orange. *Journal of Materials Science: Materials in Electronics* **28**, 14033–14039. https://doi.org/10.1007/s10854-017-7254-2.

Gita, S., Hussan, A., Choudhury, T. G., Gita, S. & Hussan, A. 2017 Impact of textile dyes waste on aquatic environments and its treatment. *Environment and Ecology* **35**, 2349–235335.

Hossain, A., Abdallah, Y., Ali, M. A., Masum, M. M. I., Li, B., Sun, G., Meng, Y., Wang, Y. & An, Q. 2019 Lemon-fruit-based green synthesis of zinc oxide nanoparticles and titanium dioxide nanoparticles against soft Rot bacterial pathogen *Dickeya dadantii*. *Biomolecules* **9**. https://doi.org/10.3390/biom9120863.

Ito, T., Adachi, Y., Yamanashi, Y. & Shimada, Y. 2016 Long-term natural remediation process in textile dye-polluted river sediment driven by bacterial community changes. *Water Research* **100**, 458–465. https://doi.org/10.1016/j.watres.2016.05.050.

Kamarajan, D., Anburaj, B., Porkalai, V., Muthuvel, A., Nedunchezhian, G. & Mahendran, N. 2022 Green synthesis of ZnO nanoparticles and their photocatalyst degradation and antibacterial activity. *Journal of Water and Environmental Nanotechnology* **7**, 180–193. https://doi.org/10.1016/j.jics.2022.100695.

Kaur, G., Kaur, H., Kumar, S., Verma, V., Jhinjer, H. S., Singh, J., Rawat, M., Singh, P. P. & Al-Rashed, S. 2021 Blooming approach: one-pot biogenic synthesis of TiO_2 nanoparticles using *Piper betle* for the degradation of industrial reactive yellow 86 dye. *Journal of Inorganic and Organometallic Polymers and Materials* **31**, 1111–1119. https://doi.org/10.1007/s10904-020-01797-y.

Khan, S. & Malik, A. 2018 Toxicity evaluation of textile effluents and role of native soil bacterium in biodegradation of a textile dye. *Environmental Science and Pollution Research* **25**, 4446–4458. https://doi.org/10.1007/s11356-017-0783-7.

Khan, M., Ware, P. & Shimpi, N. 2021 Synthesis of ZnO nanoparticles using peels of *Passiflora foetida* and study of its activity as an efficient catalyst for the degradation of hazardous organic dye. *SN Applied Sciences* **3**, 528. https://doi.org/10.1007/s42452-021-04436-4.

Mayuri, M., Asima, D. & Joseph, K. S. 2022 Phytochemical analysis and antioxidant activities of *Artemisia stelleriana* Besser leaf extracts. *Plant Science Today* **9**, 215–220. https://doi.org/10.14719/pst.1263.

Mohammadi Shivyari, A., Tafvizi, F. & Noorbazargan, H. 2022 Anti-cancer effects of biosynthesized zinc oxide nanoparticles using *Artemisia scoparia* in Huh-7 liver cancer cells. *Inorganic and Nano-Metal Chemistry* **52**, 375–386.

Mucciarelli, M. & Maffei, M. 2001 Introduction to the genus. In: *Artemisia*. CRC Press, pp. 16–57. https://doi.org/10.1201/9780203303061-8.

Mutukwa, D., Taziwa, R. & Khotseng, L. E. 2022 A review of the green synthesis of ZnO nanoparticles utilising Southern African indigenous medicinal plants. *Nanomaterials* **12**(19), 3456. https://doi.org/10.3390/nano12193456.

Nagajyothi, P. C., Prabhakar Vattikuti, S. V., Devarayapalli, K. C., Yoo, K., Shim, J. & Sreekanth, T. V. M. 2020 Green synthesis: photocatalytic degradation of textile dyes using metal and metal oxide nanoparticles-latest trends and advancements. *Critical Reviews in Environmental Science and Technology* **50**, 2617–2723. https://doi.org/10.1080/10643389.2019.1705103.

Nimbalkar, A. R. & Patil, M. G. 2017 Synthesis of ZnO thin film by sol-gel spin coating technique for H2S gas sensing application. *Physica B: Condensed Matter* **527**, 7–15. https://doi.org/10.1016/j.physb.2017.09.112.

Osuntokun, J., Onwudiwe, D. C. & Ebenso, E. E. 2019 Green synthesis of ZnO nanoparticles using aqueous *Brassica oleracea* L. var. *italica* and the photocatalytic activity. *Green Chemistry Letters and Reviews* **12**, 444–457. https://doi.org/10.1080/17518253.2019.1687761.

Panagopoulos, A. 2021 Water-energy nexus: desalination technologies and renewable energy sources. *Environmental Science and Pollution Research* **28**(17), 21009–21022. https://doi.org/10.1007/s11356-021-13332-8.

Panagopoulos, A. 2022 Brine management (saline water & wastewater effluents): sustainable utilization and resource recovery strategy through minimal and zero liquid discharge (MLD & ZLD) desalination systems. *Chemical Engineering and Processing-Process Intensification*, 108944. https://doi.org/10.1016/j.cep.2022.108944.

Panagopoulos, A. & Giannika, V. 2022 Decarbonized and circular brine management/valorization for water & valuable resource recovery via minimal/zero liquid discharge (MLD/ZLD) strategies. *Journal of Environmental Management* **324**, 116239. https://doi.org/10.1016/j.jenvman.2022.116239.

Rafiq, A., Ikram, M., Ali, S., Niaz, F., Khan, M., Khan, Q. & Maqbool, M. 2021 Photocatalytic degradation of dyes using semiconductor photocatalysts to clean industrial water pollution. *Journal of Industrial and Engineering Chemistry* **97**, 111–128. https://doi.org/10.1016/j.jiec.2021.02.017.

Sadiq, H., Sher, F., Sehar, S., Lima, E. C., Zhang, S., Iqbal, H. M., Zafar, F. & Nuhanović, M. 2021 Green synthesis of ZnO nanoparticles from *Syzygium cumini* leaves extract with robust photocatalysis applications. *Journal of Molecular Liquids* **335**, 116567.

Umamaheswari, A., Prabu, S. L., John, S. A. & Puratchikody, A. 2021 Green synthesis of zinc oxide nanoparticles using leaf extracts of *Raphanus sativus* var. *Longipinnatus* and evaluation of their anticancer property in a549 cell lines. *Biotechnology Reports* **29**, e00595. doi:10.1016/j.btre.2021.e00595.

Vinayagam, R., Selvaraj, R., Arivalagan, P. & Varadavenkatesan, T. 2020 Synthesis, characterization and photocatalytic dye degradation capability of *Calliandra haematocephala*-mediated zinc oxide nanoflowers. *Journal of Photochemistry and Photobiology B: Biology* **203**, 111760. https://doi.org/10.1016/j.jphotobiol.2019.111760.

Yashni, G., AlGheethi, A., Maya Saphira Radin Mohamed, R., Nor Hidayah Arifin, S., Abirama Shanmugan, V. & Hashim Mohd Kassim, A. 2020 Photocatalytic degradation of basic red 51 dye in artificial bathroom greywater using zinc oxide nanoparticles. *Materials Today: Proceedings* **31**, 136–139. https://doi.org/10.1016/j.matpr.2020.01.395.

First received 12 January 2023; accepted in revised form 11 March 2023. Available online 27 March 2023